Monte Carlo study of phase transitions and magnetic properties of $LaMnO_3$

S. Naji [a,b], A. Benyoussef [a,c,d], A. El Kenz [a], H. Ez-Zahraouy [a] and M. Loulidi [a]

[a] LMPHE (URAC 12), Département de physique, Faculté des sciences, Université Mohammed V-Agdal, B.P. 1014, Rabat, Morocco

[b] Department of Physics, faculty of sciences, IBB university , Ibb , Yemen

[c] Hassan II Academy of Sciences and Technology, Rabat, Morocco

[d] Institute of Nanomaterials and Nanotechnology, MAScIR, Rabat, Morocco

Abstract:

On the basis of Mean Field Approximation (MFA), Monte Carlo Simulations (MCS) and ab initio calculations we have studied the phase diagrams and magnetic properties of the bulk perovskite, LaMnO3 using Ising model Hamiltonian. It is shown that the antiferromagnetic coupling between next neighbors Mn ions is reponsible for a series of magnetic phase transitions. The transition temperature and the critical exponents obtained, in the framework of Monte Carlo simulations, using the experimental values of the exchange couplings and magnetic anisotropy are in agreement with the experimental ones. The exchange couplings deduced from ab initio calculations lead, by using Monte Carlo simulations, to a quantitative agreement with the experimental transition temperatures.

I-Introduction

The $LaMnO_3$ is a member of a very large family of inorganic crystalline solids called perovskite that has the formula ABO_3 where A is large cation with different valence and B is transition metal. Since more than six decades, the parent perovskite $LaMnO_3$ and its compounds have been studied [1-4]. However, after the discovery of the magneto resistance[5] several studies have been renewed interest intensively, during the last years, in the perovskite manganese oxides especially $LaMnO_3$ which is considered as the parent of the negative colossal and tunnel magneto-resistance compounds with the general formula $La_{1-x}D_xMnO_3$ where D is divalent alkaline earth ions, such as Ca^{2+}, Sr^{2+} , Ba^{2+}[5-10], and also in the field of magnetic refrigerators, the magneto-caloric properties of the compounds $La_{0.7}Ca_{0.3-x}K_xMnO_3$ are strongly recommended to use as an active magnetic refrigerant near room temperature [11,12]. Furthermore the $LaMnO_3$ materials have a significant interest for cathode and electrolyte of solid oxide fuel cell (SOFCs) [13].

The interesting physical properties and the rich phase diagrams of doped and undoped $LaMnO_3$ result from the strong interplay between the different degrees of freedom lattice, spin, charge, and orbital [14,15]. These phase diagrams may present different states namely an anti-ferromagnetic (AF) insulator, ferromagnetic (F) metal, or charge-ordered (CO) insulator, depending on the doping concentration, pressure, and temperature [16]. In particular, the parent $LaMnO_3$ in which Mn^{3+} is the only present high spin magnetic ion , S =2 (t^3_{2g} e^1_g), is an antiferromagnetic (*A*-type) whose Neel temperature is T_N=139.5 K , insulator with an energy of gap1.7 eV , and it shows also an orbital ordering (*C*-type) below 780 K. The Jahn-Teller electronic ordering couples the Mn^{3+} spins within the basal planes with a ferromagnetic coupling (super exchange interaction). These planes are coupled one to another with an antiferromagnetic coupling [17-19].

The crystallographic structure of $LaMnO_3$ is distorted from the ideal cubic structure and stabilizes in the orthorhombic one. This is due to two effects namely the size difference between the cations La and Mn, which is represented by the tolerance factor of Gold Schmidt, and the Jahn-Teller effect.

At our knowledge, even though several theoretical and experimental studies have been made on this material. Neither the magnetic properties nor the phase diagram of $LaMnO_3$ have been investigated theoretically using different methods of statistical physics such as Monte Carlo simulations(MCS), mean field approximation(MFA), and ab initio calculations (AKAI-KKR) together.

In this work, we use the methods mentioned above (MCS, MFA, ab initio) to study the phase diagrams and magnetic properties of the bulk perovskite $LaMnO_3$ in the framework of Ising model. We restricted ourselves to the values of exchange couplings that are deduced on the one hand from ab initio calculations and on the other hand from experiment [19]. The magnetic susceptibility and critical exponents are computed only within MCS. Thus, in section II we give the structure and the model of the bulk $LaMnO_3$ while in section III we study the magnetic properties and present the phase diagram of our compound. The ab initio calculation of the exchange couplings is given in Section IV and Section V is reserved to the conclusion.

II- Structure and Model

The experiments of neutron diffraction [19] at temperature T= 1.4 K show that the bulk perovskite $LaMnO_3$ has an orthorhombic structure with space group 62 pnma and has a unit cell with lattice parameters a= 5.5333 Å, b= 5.7461 Å and c= 7.6637 Å. The atoms and Wyckoff positions are Mn in 4b (0.5, 0, 0), La in 4c (-0.0095, 0.0513, 0.25), $O_{(1)}$ in 4c (0.0777, 0.48493, 0.25), and $O_{(2)}$ in 8d (0.7227, 0.3085, 0.0408). According to these experiments the dispersion of the spin waves satisfies the following Hamiltonian model:

$$H = -2J_1\sum_{i>j} S_i S_j - 2J_2\sum_{i>k} S_i S_k - \Delta\sum_i (S_i)^2$$

where J_1(F)= 9.6 K(0.83 meV) is the exchange coupling between the nearest neighbors manganese ions in the basal planes, J_2(AF)= - 6.7K (- 0.58 meV) the exchange coupling between the next nearest neighbors manganese ions between these planes and Δ =1.92K (0.165 meV) the magnetic anisotropy.

III--phase diagram and magnetic properties

The magnetic properties and the critical temperatures as function of the parameters of the model are studied using both MFA and MCS while the critical behavior of LaMnO3 and the size effects on different physical quantities are determined using MCS only.

III-1 Mean field analyzis

Even though the MFA neglects all spin correlations, it remains a power tool to study complex spin systems [20, 21] as the bulk $LaMnO_3$. The variational principle based on the Gibbs–Bogoliubov inequality for the free energy per site of a system of N atoms is described by [22, 23]:

$$F \le F_0 = \frac{-T}{N}\ln(Z_0) + \frac{1}{N}\langle H - H_0\rangle_0 \quad (1)$$

where H is the hamiltonian of the system, H_0 an effective hamiltonian in which the interactions of each spin S_i with its neighbors are assimilated to an effective field h and Z_0 is the associated partition function. The symbol $< .. >_0$ denotes the thermal average obtained with the effective hamiltonian H_0. Since the next nearest neighbor Mn ions interact antiferromagnetically, the whole lattice is divided into two magnetic sublattices I and II and the Hamiltonian of our system is given by:

$$H = -J_1\sum_{i,j\in I} S_i^z S_j^z - J_2\sum_{i\in I, j\in II} S_i^z S_j^z - \Delta\sum_{i\in I}(S_i^z)^2 - J_1\sum_{i,j\in II} S_i^z S_j^z - \Delta\sum_{i\in II}(S_i^z)^2 \quad (2)$$

where $S^z = \pm 2, \pm 1, 0$ is the z component of the spin S=2 of Mn^{3+}. The effective Hamiltonian of the system is:

$$H_0 = h_I\sum_{i\in I}^{N} S_i + h_{II}\sum_{i\in II}^{N} S_i - \Delta\sum_{i\in I}^{N} S^2 - \Delta\sum_{i\in II}^{N} S^2 \quad (3)$$

where the effective fields h_I and h_{II} are given by:

$$h_I = -J_1\sum_{j\in I}^{z_1} < S_j >_0 - J_2\sum_{k\in II}^{z_1} < S_k >_0 = -J_1 z_1 m_I - J_2 z_2 m_{II} \quad (4)$$

$$h_{II} = -J_1\sum_{j\in II}^{z_1} < S_j >_0 - J_2\sum_{k\in I}^{z_1} < S_k >_0 = -J_1 z_1 m_{II} - J_2 z_2 m_I \quad (5)$$

z_1 = 4 and z_2 = 2 denote the number of nearest neighbors and next nearest neighbors respectively in each sublattice and m_I = $<S_j>_{j\in I}$ and m_{II} = $<S_j>_{j\in II}$ are the order parameters of the system. The effective Hamiltonian H_0 generates the partition function

$$Z_0 = Tr\left(e^{\frac{-H_0}{T}}\right) = \left(\left(e^{\frac{4\Delta}{T}} 2\cosh\left(\frac{2h_I}{T}\right) + e^{\frac{\Delta}{T}} 2\cosh\left(\frac{h_I}{T}\right) + 1\right)\left(e^{\frac{4\Delta}{T}} 2\cosh\left(\frac{2h_{II}}{T}\right) + e^{\frac{\Delta}{T}} 2\cosh\left(\frac{h_{II}}{T}\right) + 1\right)\right)^N \quad (6)$$

Following the variational principle, the free energy

$$F_0 = -\frac{T}{N}\ln(Z_0) - \frac{z_1}{2}J_1 m_I^2 - \frac{z_1}{2}J_1 m_{II}^2 - \frac{z_2}{2}J_2 m_I m_{II} - h_I m_I - h_{II} m_{II} \quad (7)$$

is minimized to obtain the order parameters m_I and m_{II}, which are the magnetizations of the two sublattices. The equations of state of the system are then given by:

$$m_I = \frac{(e^{\frac{4\Delta}{T}} 4\sinh(\frac{2h_I}{T}) + e^{\frac{\Delta}{T}} 2\sinh(\frac{h_I}{T}))}{(e^{\frac{4\Delta}{T}} 2\cosh(\frac{2h_I}{T}) + e^{\frac{\Delta}{T}} 2\cosh(\frac{h_I}{T}) + 1)} \quad (8a)$$

$$m_{II} = \frac{(e^{\frac{4\Delta}{T}} 4\sinh(\frac{2h_{II}}{T}) + e^{\frac{\Delta}{T}} 2\sinh(\frac{h_{II}}{T}))}{(e^{\frac{4\Delta}{T}} 2\cosh(\frac{2h_{II}}{T}) + e^{\frac{\Delta}{T}} 2\cosh(\frac{h_{II}}{T}) + 1)} \quad (8b)$$

The solutions of the self consistent equations (8) are not unique, the stable ones are those minimizing the free energy F_0 (eq. 7) while the others are the unstable ones. If the order parameters are continuous (discontinuous), the transitions are of second (first) order.

First, it would be useful to study the ground state phase diagram of our system which is described by the Hamiltonian (1) and represented in figure (1). Such ground state phase diagram is established according to the calculations of all possible configurations energies being in the two sublattices and compared between them. Thus, depending on the parameters $r = J_2/J_1$ and $d = \Delta/2J_1$ different phases may occur namely: the antiferromagnetic phase AF_2 (A-type) ($m_I = 2$, $m_{II} = -2$), the ferromagnetic phase F_2 ($m_I = 2$, $m_{II} = 2$) and the disordered phase D ($m_I = 0$, $m_{II} = 0$) which are stable in a range of the plane (r , d) while the the ferromagnetic phase F_1 ($m_I = 1$, $m_{II} = 1$) and the antiferromagnetic phase AF_1 ($m_I = 1$, $m_{II} = -1$) are stable only along the transition lines. A first order transition where both antiferromagnetic phases AF_2 and AF_1 and the disordered phase coexist is located at line $d = r - 2$ for $r < 0$ and $d < -2$ ($J_1 > 0$). Since the phase diagram is symmetrical with regard to $r = 0$, one obtains a first order transition line at $d = -r - 2$ where all ferromagnetic phases and the disordered phase coexist. The AF_2-AF_1 phase transition occurs at $r = 0$. As seen clearly, for the experimental values $r \approx -0.7$ and $d = 0.1$ [19], the bulk perovskite $LaMnO_3$ is in the antiferromagnetic AF_2 (A-type) phase.

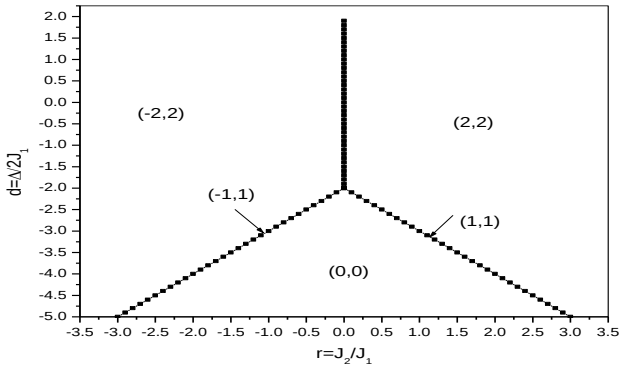

Figure 1: The ground-state phase diagram of the bulk perovskite $LaMnO_3$ model represented in the ($r = J_2/J_1$, $d = \Delta/2J_1$) plane

At non vanishing temperature, the magnetic properties of the the bulk perovskite $LaMnO_3$ are deduced from the equations of state (eq. 8). The stable solutions are those which minimize the free energy F_0 (eq. 7). In what follow, we will restrict ourselves to the parameters that correspond to the experimental values of $LaMnO_3$. The total magnetization of the system is then defined as:

$$m = \frac{|m_I - m_{II}|}{2} \quad (9)$$

In figure (2), the behavior of the magnetization m(T) is ploted as function of the temperature for the experimental values of $LaMnO_3$ ($r = 0.697$, ***d*=0.1**). It is shown that m vanishes continuously at a critical temperature $T_c = 210$K, which is greater than the experimental one **(T_{exp}=139.5K)**. This desagreement is due to the fact that in the MFA all spin correlations are neglected. Thus, the bulk perovskite $LaMnO_3$ exhibits a second order phase transition at a finite critical temperature.

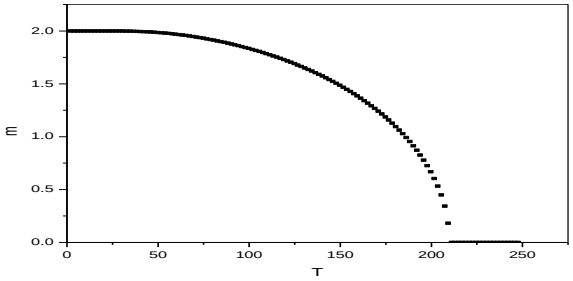

Figure 2: The magnetization of $LaMnO_3$ as a function of the temperature for r =0.697, **d=0.1**

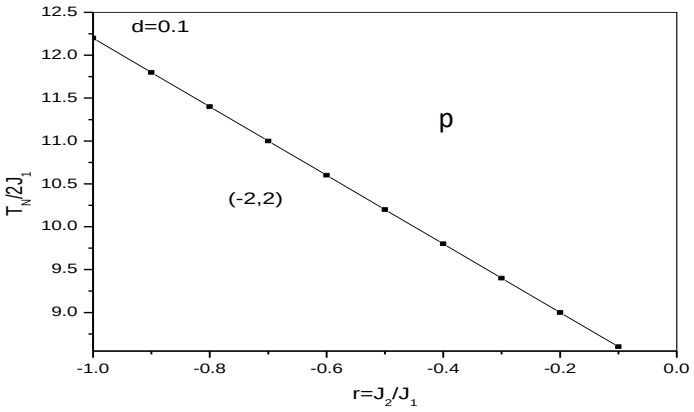

Figure 3: The reduced transition temperatures as a function of r

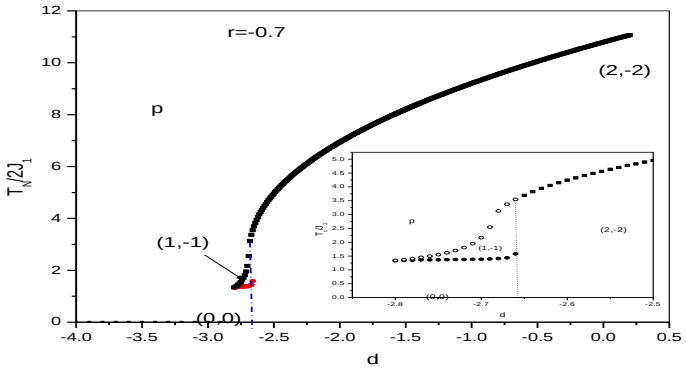

Figure 4: The reduced transition temperature as a function of d. The dashed lines represent first-order transitions

In order to show the effect of different parameters on the phase diagram and transition temperatures, we present in figure 3 the reduced transition temperature as a function of the reduced exchange coupling *r* for the experimental value of the reduced magnetic anisotropy ***(d=0.1)***. At this value of *d*, the system undergoes a second order phase transition between AF_2 and the paramagnetic phase P and the critical temperature decreases by increasing the reduced coupling *r*. On the other hand the effect of the reduced magnetic anisotropy *d* is presented in figure 4 for the experimental value of the reduced exchange coupling *r*. We show that the AF_1, which is stable for vanishing temperature (T=0) only at the critical line (see fig. 1), extends its region of stability in a certain interval of *d*. Moreover, the thermal excitations may stabilize the AF_1 phase for all values of $d < -2$. The AF_1—AF_2 and AF_2—D transitions are of first order while the transitions AF_1—P and AF_2—P are of second order. Finally in fig (5),we plot the behavior of the magnetization as a function of the reduced temperature for d=-2.7 and r =-0.7 in which The two lines show the transition from the phase (2,-2) to the phase (1,-1) and the order-disorder transition.

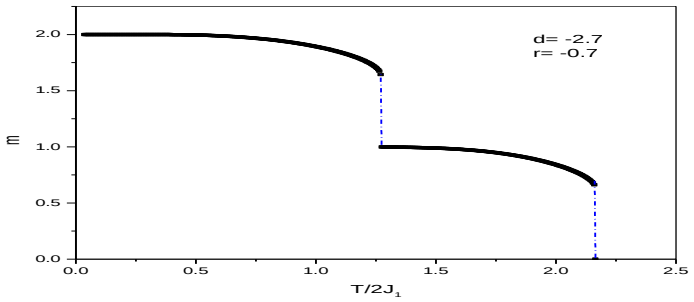

Figure 5: The dependence of the magnetization as a function of the reduced temperature for d=-2.7 and the dashed lines represent first-order transition.

III-2 Size effects on magnetic properties of $LaMnO_3$ and the critical behavior

In order to investigate the critical behavior and the size effects on magnetic properties of our model we develop MCS, which are more appropriate for calculating thermal equilibrium properties and critical exponents for complex systems. We used the Metropolis algorithm to compute the thermodynamic quantities of interest. Thus, the magnetization, the magnetic susceptibility and the specific heat are given respectively by:

$$m = \frac{1}{N}\left|\sum_{i\in I} S_i - \sum_{i\in II} S_i\right| \tag{10}$$

$$\chi = \frac{2N}{K_B T}\left(\left\langle m^2\right\rangle - \left\langle m\right\rangle^2\right) \tag{11}$$

$$C_v = \frac{1}{2N(K_B T)^2}\left(\left\langle E^2\right\rangle - \left\langle E\right\rangle^2\right) \tag{12}$$

where *E* is the internal energy of the system, K_B is the Boltzmann's constant and $N = L^d/2$ is the number of spin in each sublattice.

The critical behavior of these observables quantities is given by :

$$m\alpha(T - T_c)^{\beta} \tag{13}$$

$$\chi\alpha\left|T - T_c\right|^{-\gamma} \tag{14}$$

$$C_v \alpha |T - T_c|^{-\alpha} \quad (15)$$

where β , γ and α are the associated critical exponents. According to the scaling law:

$$Q(t,L) = L^{y/\nu} f(t/L^{-1/\nu}) \quad (16)$$

where f is a scaling function, t = T-T_c , and y =-β for $Q(t,L)$ = $m(t,L)$, y = γ for $Q(t,L)$ = $\chi(t,L)$ and y = α for $Q(t,L)$ = $C_v(t,L)$, the lattice size dependence of the thermal quantities at critical temperature are given by:

$$M_{T_c}(L) \alpha L^{-\frac{\beta}{\nu}} \quad (17)$$

$$\chi^{\max}(L) \alpha L^{\frac{\gamma}{\nu}} \quad (18)$$

$$C^{\max}(L) \alpha L^{\frac{\alpha}{\nu}} \quad (19)$$

The magnetic properties and the critical behavior of the bulk perovskite $LaMnO_3$ are investigated for systems with linear size L varying from L=4 to L=40. We note that L=28 is the thermodynamical limit above which the behavior of the thermal quantities and the transition temperature do not change.

According to the experimental values of the bulk perovskite $LaMnO_3$ parameters, the variation of the magnetization and the susceptibility as function of the temperature for different system sizes are plotted in figure 6. The magnetization vanishes continuously at critical temperature indicating that the transition is of second order. The peak of the susceptibility and its corresponding temperature increase by increasing the lattice size L before reaching the critical transition temperature T_c=171°K for a sufficiently large value of L. In figure 7, we present the reduced transition temperature dependence of the reduced exchange coupling r for the experimental value of the reduced magnetic anisotropy $d=0.1$ for L=28. The reduced transition temperature decreases when the reduced exchange coupling r increases, which is in agreement with the result obtained with the MFA. The effect of the magnetic anisotropy on the phase diagram for the experimental value of the reduced coupling $r=-0.7$ is shown in figure 8. It is qualitatively in agreement with the one obtained with the MFA, except that the thermal excitations may stabilize the AF_1 phase only on the first order transition line.

Since the critical temperature is not obtained with very high accuracy, the critical exponents β, γ, and α are computed according to the finite size scaling relations (eq. 17-19). By using the theoretical value of the critical exponent ν associated to the correlation length ξ ($\xi \sim t^{-\nu}$) **ν=0.625 [31]**, we obtain β=0.29869±0.0247, which is very close to the experimental value(β=0.316) [32], and to the theoretical value of the three dimentional Ising model (β=0.32) **[32]**. The critical exponent γ =1.2857 ±0.02648 and α = 0.1386±0.03662 we obtain are close to the theoretical ones **[32]**.

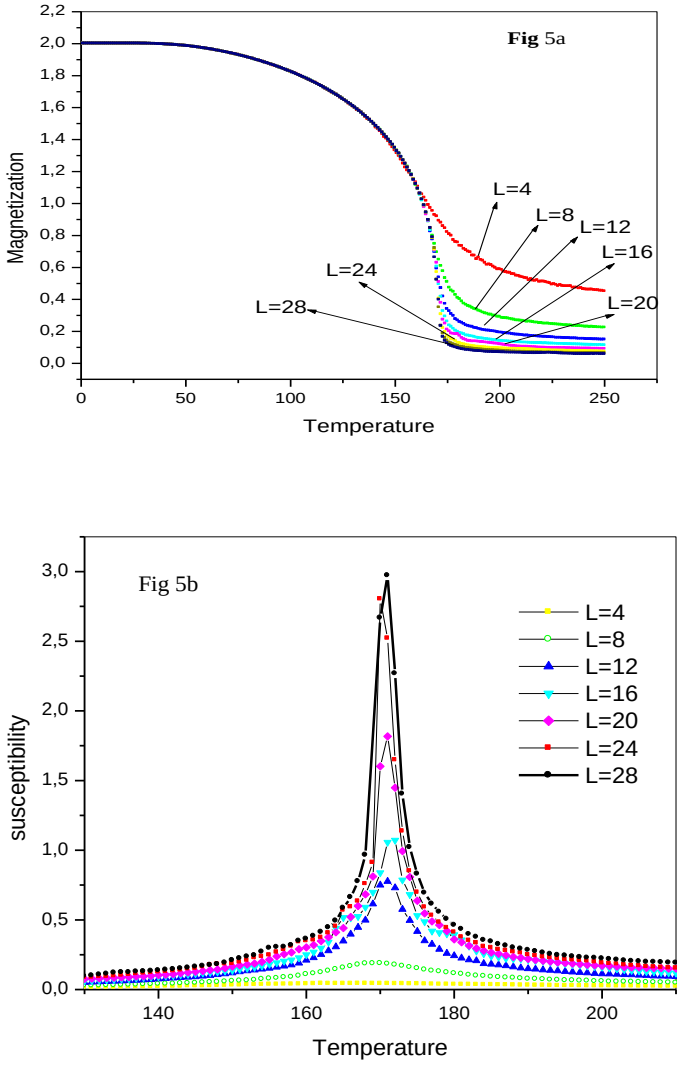

Figure 6: a- the magnetization and b- the susceptibility as a function of the temperature for different system sizes ranging from L=4 to L=28

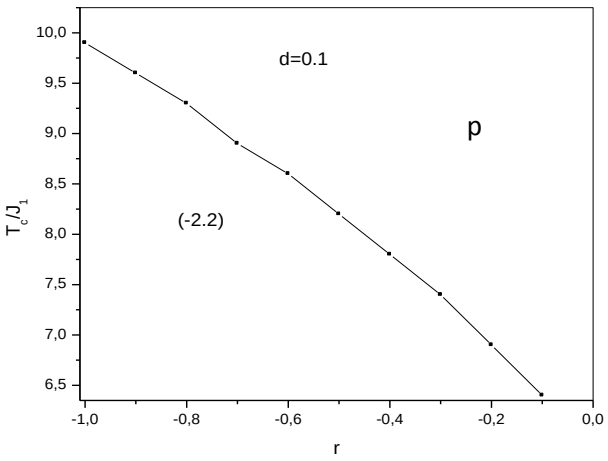

Figure 7: The transition temperatures as a function of r for d=0.1and a system size L =28

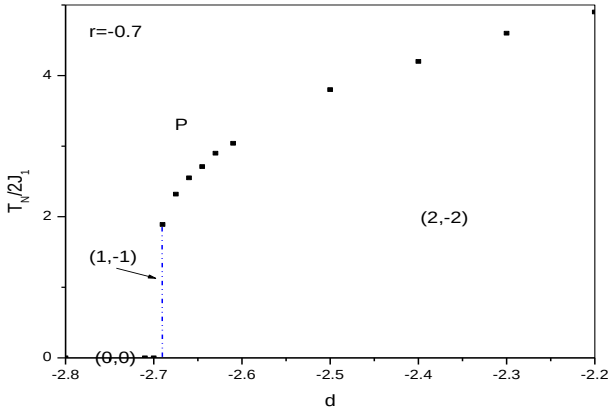

Figure 8: The transition temperatures as a function of d and for r=-0.7and system size L =28. The dashed lines represent first-order transitions

IV-Ab-initio calculation: exchange couplings values

In order to find the exact theoretical values of the exchange couplings and the magnetic moment of the bulk perovskite $LaMnO_3$, we have used ab initio calculation based on the Korringa–Kohn–Rostoker (KKR) Green's function method and the parameterization methods of the exchange energy VBH[25],VWN[26], MJW[27], GGA[28], EV[29] combined with the atomic sphere approximation(ASA). To solve the Density Functional Theory (DFT) one-particle equations one use multiple-scattering theory, i.e. the KKR Green's function (KKR-GF) method. The relativistic effect is taken into account by employing the scalar relativistic approximation. The form of the crystal potential is approximated by a muffin-tin potential, and the wave functions in the respective muffin-tin spheres were expanded in real harmonics up to l=6, where l is the angular momentum quantum number defined at each site. 201K-points in the irreducible part of the first Brillouin zone are used in our calculation. For the present KKR-CPA calculations, we use the package MACHIKANEYAMA2000 coded by Akai [30]. The bulk perovskite $LaMnO_3$ has an orthorhombic structure with space group 62 pnma and has a unit cell with lattice parameters a= 5.5333 Å, b= 5.7461 Å and c= 7.6637 Å. The atoms and Wyckoff positions are Mn in 4b (0.5, 0, 0), La in 4c (-0.0095, 0.0513, 0.25), $O_{(1)}$ in 4c (0.0777, 0.48493, 0.25), and $O_{(2)}$ in 8d (0.7227, 0.3085, 0.0408).

The exchange couplings are calculated from the energy difference between the four magnetic configurations:
(A-AF), which corresponds to ferromagnetic exchange coupling $J_1 > 0$ and antiferromagnetic exchange couplings $J_2 < 0$, (C-AF) in which $J_1 < 0$ and $J_2 > 0$, (G-AF) where both J_1 and J_2 are antiferromagnetic and (F), which is obtained for ferromagnetic exchange couplings $J_1 > 0$ and $J_2 > 0$. Therefore, according to the Hamiltonian (1), the two unknown exchange couplings J_1 and J_2 may be obtained by using the following equations:

$$J_1 = \frac{E(C-AF)-E(F)}{32m^2},$$

$$J_2 = \frac{E(A-AF)-E(F)}{16m^2}$$

where m is the Mn ions magnetic moment and E(A-AF), E(C-AF) and E (F) are the total energy of $LaMnO_3$ in the corresponding magnetic configurations (Table 1).
The total density of states (DOS) in the different magnetic configurations ferromagnetic (F), antiferromagnetic A-type (A-AF), C-type (C-AF) and G-type (G-AF) are presented in figure 9. The important factors governing the formation of the electronic structure of orthorhombic $LaMnO_3$ are the exchange splitting owing to spin polarization. It is believed that LaMnO3 is a charge-transfer-type insulator [33-35] according to the Zaanen-Sawatzky-Allen scheme, in which the lowest-lying gap transition correspond to the charge-transfer excitation from the O 2p to Mn 3d state and has four d electrons per Mn3+ site with a configuration of $t^3_{2g}\ e^1_g$. Figure 9a show insulating behavior in the A-AF phase of LaMnO3. The valence-band are derived from Mn 3d and O 2p admixture with dominant Mn 3d character. Valence band of A-AF phase of orthorhombic LaMnO3 is generally composed of four regions. The lowest-energy region contains mainly O 2*s* bands; above this, the La 5*p* bands.

Both the O 2s and La 5p bands are well separated from the bands in the vicinity of E_F, and consequently they hardly contribute to the chemical bonding or to transport properties. The O 2p bands degenerate with the Mn 3d states in the whole valence band region, indicating covalent interactions between Mn and O in LaMnO3. The top of valence band is dominated by the majority spin Mn 3d states, indicating the importance of Mn 3d states in transport properties such as colossal magnetoresistance observed in hole-doped LaMnO3. The bottom of the conduction band is dominated by the minority-spin Mn 3d electrons, and above the La 4 f electrons are present in a very narrow energy range.

Moreover, the value of the magnetic moment obtained is ($3.54\mu_B$), which is smaller than the experimental one ($3.8\mu_B$). This indicate that the Mn ions are in the high-spin state and hence the contributions to the minority-spin channel from the Mn 3d electrons are negligibly small.

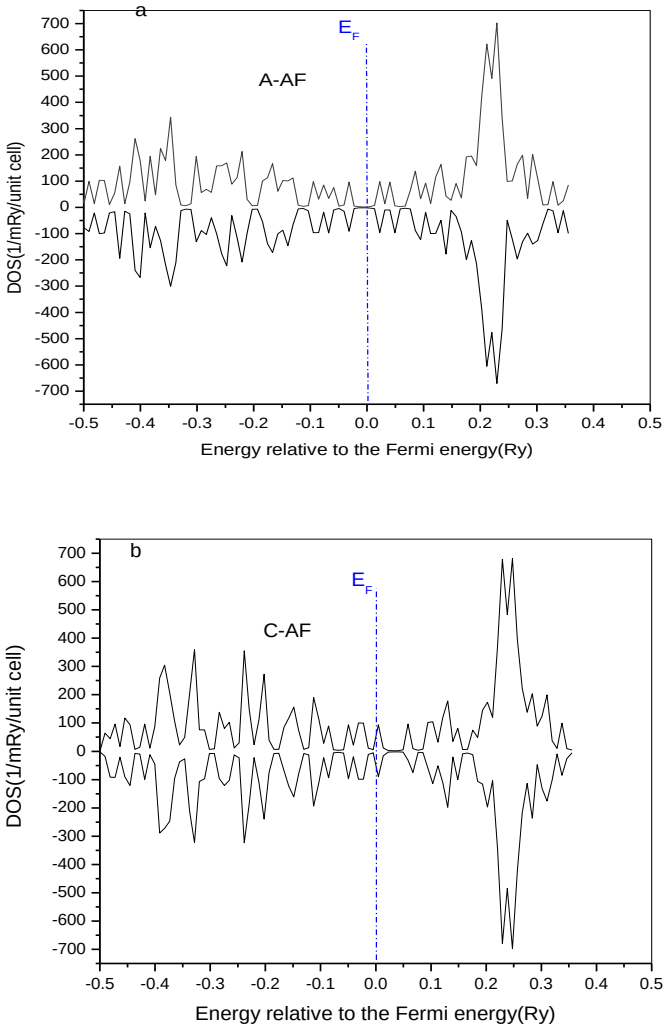

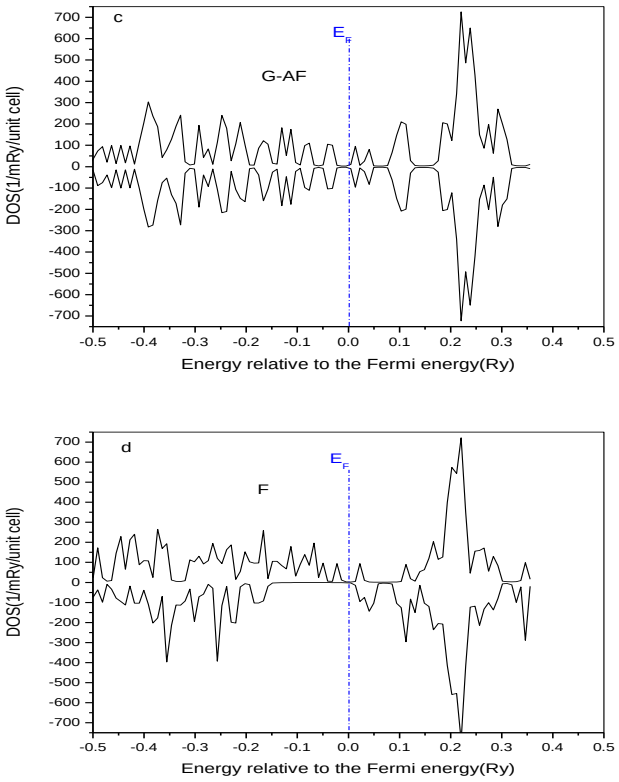

Figure 9: Total DOS of $LaMnO_3$ in magnetic configurations a-(A-AF), b-(C-AF), c-(G-AF) and d-(F) by GGA method.

According to the calculations of the values of the exchange couplings for several parameterization methods, it is found that the exchange couplings values obtained by the GGA methods are J_1= 0.87 meV and J_2= -0.60 meV. They are very close to the experimental ones. Thus by substiting these values in the phase diagrams that have been obtained by MCS and MFA we obtain the coresponding transition temperature T_c = 169.7K and T_c = 208 K, respectively. The transition temperature obtained by MCS is close to the experimental one (Tcexp=139.5K).

E(F) *(Ry)*	E(A-AF) *(Ry)*	E(C-AF) *(Ry)*	E(G-AF) *(Ry)*
-79037.5456856	-79037.5545646	-79037.5200747	-79037.5111200

Table 1. The total energy in (Ry) of $LaMnO_3$ in magnetic configurations (F), (A-AF), (C-AF) and (G-AF) by the GGA method.

V- Conclusion

In this work we have investigated, using MCS, MFA and ab initio calculations, the phase diagrams and magnetic properties of the bulk perovskite $LaMnO_3$ for different

values of the phase space parameters. Different antiferromagnetic phases were observed and the system exhibits second order as well as a first order transitions depending on the value of the reduced magnetic anisotropy. According to the experimental values of the exchange couplings and the magnetic anisotropy we have shown that $LaMnO_3$ exhibits a second order-disorder phase transition at a critical temperature T_c = 171.1°K. The size effects were studied using MCS and the critical exponents associated to the magnetization, the susceptibility and the specific heat were calculated. They are in agreement with the experimental ones. In addition we have shown that the exchange couplings deduced from ab initio calculations are in agreement with the experimental ones. They lead to a critical temperature T_c= 169.7°K, which is of order to the one obtained experimentally.

References

1- G.H. Jonker and J.H. Van Santen. Physica 16 Physica, 16, Issue 3, p.337-349, (1950),

2- G.H. Jonker ,Physica, 22, Issues 6-12, p.707-722

3- E. O. Wollan and W. C. Koehler, Phys. Rev. 100, 545 (1955)

4- C. Zener,Phys. Rev. 82, 403–405 (1951)

5- M. N. Baibich,J. M. Broto, A. Fert, F. Nguyen Van Dau, F. Petroff, P. Eitenne, G. Creuzet, A.Friederich, and J. Chazelas, Phys Rev Lett.61 (21), 2472. (1988)

6- R. von Helmolt, J. Wecker, B. Holzapfel, L. Schultz, and K. Samwer, Phys. Rev. Lett.71 (21), 2331.(1993)

7- S. Jin, T. H. Tiefel, M. McCormack, R. A. Fastnacht, R. Ramesh and L. H. Chen Science 264, 413(1994)

8- Ju H. L., Kwon C., Li Qi, Greene R. L. and Venkatesan T. Appl. Phys. Lett. 65, 2108(1994)

9- J. Fontcuberta, B. Martínez, A. Seffar, S. Piñol , A.Roig, E. Molins, X.Obradors, J.Alonso and J. M. González-Calbet, J. Appl. Phys. 79, 5182(1996)

10- M. Bowen,M. Bibes, A. Barthélémy, J.-P. Contour, A. Anane, Y. Lemaître and A. Fert ,Appl. Phys. Lett. 82, 233 (2003)

11- M. Bejar , R. Dhahri , E. Dhahri , M. Balli and E.K. Hlil, J. Alloys Compd. 442 (2007) 136–138

12- M. Bejar , E. Dhahri , E.K. Hlil and S. Heniti , J. Alloys Compd. 440 (2007) 36–42

13- C. Monterrubio-Badillo, H. Ageorges, T. Chartier, J.F. Coudert, P. Fauchais , J.Surfcoat 200 (2006) 3743 – 3756

14- O. Satoshi,I.Sumio and M. Sadamichi , Phys. Rev. B 65, 144403 (2002)

15- T. Mizokawa, D. I. Khomskii, and G. A. Sawatzky Phys. Rev. B 60, 7309–7313 (1999)

16- P. Schiffer, A. P. Ramirez, W. Bao, and S-W. Cheong , Phys. Rev. Lett. 75, 3336–3339 (1995)

17- 5Y. Murakami, J. P. Hill, D. Gibbs, M. Blume, I. Koyama, M.Tanaka, H. Kawata, T. Arima, Y. Tokura, K. Hirota, and Y. Endoh, Phys. Rev. Lett. 81, 582 (1998)

18- J . B. GOODENOUGH, Phys. Rev 100 , 564 (1955)

19- F. Moussa, M. Hennion, J. Rodriguez-Carvajal, and H. Moudden, L. Pinsard and A. Revcolevschi , Phys. Rev B54 15149, (1996)

20- L. Bahmad, A. Benyoussef, and A. El Kenz, Phys. Rev B **76**, 094412 (2007)

21- L. Bahmad, A. Benyoussef, and A. El Kenz, physica A 387, (2008)

22- N.N. Bogoliubov, J. Phys. (USSR) 11 (1947) 23.

23- R.P. Feynmann, Phys. Rev. 97 (1955) 660.

24- K.Binder and D.W. Heermann, Monte Carlo Simulation in Statistical Physics: An Introduction, Springer,(2002); H.T.Diep,physique de la matière condonsé ,Dunod,(2003);J. M. Yeomans ,Statistical Mechanics of Phase Transitions, Oxford,(1993).

25- U. v. Barth and L. Hedin; J. Phys. C: Solid State Phys. 5, 1629 (1972)

26- S. H. Vosko, L. Wilk, and M. Nussair; Can. J. Phys. 58, 1200 (1980); S. H. Vosko and L. Wilk; Phys. Rev. B 22, 3812 (1980).

27- V. L. Moruzzi, J. F. Janak, and A. R. Williams; Calculated Properties of Metals, Pergamon Press, New York (1978).

28-J. P. Perdew, J. A. Chevary, S. H. Vosko, K. A. Jackson, M. R. Pederson, D. J. Singh, and C. Fiolhais; Phys. Rev. B 46, 6671 (1992).

29- E. Engel and S. H. Vosko; Phys. Rev. B 47, 13164 (1993).

30-MACHIKANEYAMA2002v09: H. AkaiDepartment of Physics, Graduate School of Science, Osaka University, Machikaneyama 1-1, Toyonaka 560-0043,Japan. akai@phys.sci.osaka-u.ac.jp.

31- B.G. Nickel, *Physica* 106A (1981) 48.

32- C.F. Baillie, R. Gupta, K.A. Hawick and G.S. Pawley, *Phys. Rev.* B45 (1992) 10438, and references therein

33- T. Saitoh, A. E. Bocquet, T. Mizokawa, H. Namatame, A. Fujimori, M. Abbate, Y. Takeda, and M. Takano, Phys. Rev. B **51**, 13 942 (1995)

34- T. Arima, Y. Tokura, and J. B. Torrance, Phys. Rev. B **48**, 17 006 (1993)

35- P. Ravindran, A. Kjekshus, H. Fjellva°g, A. Delin, and O. Eriksson, Phys. Rev. B, 65, 064445 (2002)